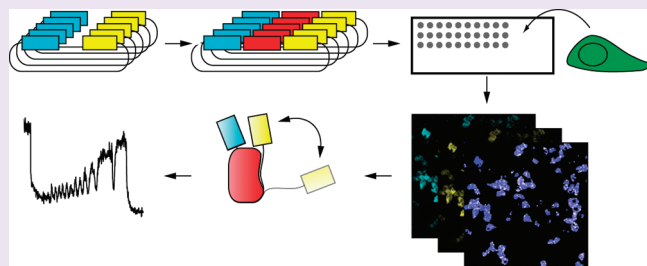


Rapid Development of Genetically Encoded FRET Reporters

Alen Piljić,[†] Iñaki de Diego,[‡] Matthias Wilmanns,[‡] and Carsten Schultz^{†,*}[†]European Molecular Biology Laboratory (EMBL), Cell Biology & Biophysics Unit, Meyerhofstrasse 1, 69117 Heidelberg, Germany[‡]European Molecular Biology Laboratory (EMBL) Hamburg, c/o DESY, Notkestrasse 85, 22603 Hamburg, Germany

S Supporting Information

ABSTRACT: To meet the demand on genetically encoded reporter molecules for live cell imaging, we introduce a new facile combined cloning and FRET reporter analysis strategy. The versatile and fully orthogonal cloning approach involves a set of up to 36 vectors featuring a variety of fluorescent protein FRET pairs and different length linkers. The construct set was successfully applied to two calmodulin-binding proteins, the death-associated protein kinase 1 (DAPK1) and calcium/calmodulin-dependent protein kinase II α (Camk2a). Clone analysis and reporter validation was performed by printing plasmid DNA arrays and subsequent semiautomated microscopy of reversely transfected cells. Characterization of the best performing DAPK1 and Camk2a reporters revealed significant differences in translating calcium signals into kinase responses despite the close functional and structural similarity.



Fluorescent protein tagging is a common method for studying proteins of interest in living cells.¹ The method aids the visualization of protein localization and spatial dynamics. Proteins tagged with two fluorescent proteins are often developed into even more powerful tools. If the two fluorescent proteins are flanking the protein of interest and their spectral properties are permissive of fluorescence resonance energy transfer (FRET), the construct has the potential to report on the protein's oligomerization and conformational status, which may be influenced by post-translational modifications, interactions with other proteins, binding of second messengers or other small-molecules and, most importantly, may reflect enzyme activity.² While being highly desirable tools for many biological problems, such conceptually simple ratiometric FRET reporters are often difficult to generate. The reason is that their performance delicately depends not only on the distance between the fluorophores but also on the orientation of their transition dipole moments.^{3,4} The latter may be altered by using differently connected fluorescent proteins, namely, circularly permuted variants.³ However, even with good structural information, correct predictions regarding sensor performance are hard to come by. Therefore, it is still a tedious process to achieve useful sensor performance. The goal of this work was to establish a rapidly implementable universal strategy for the generation and optimization of genetically encoded FRET sensors that can be handled with limited manual labor. This concept was applied to generate sensors for two structurally related calcium-calmodulin dependent kinases, death-associated protein kinase 1 (DAPK1) and calcium/calmodulin dependent protein kinase II α (Camk2a). On the basis of structural information,^{5–7} both proteins were expected to undergo major conformational changes upon calmodulin binding.

We designed a library-based workflow in which a set of backbone plasmids was prepared that contained various combinations of fluorescent donor and acceptor proteins. The kinase sequences were inserted into the backbones resulting in a FRET reporter library (Figure 1a). The plasmid DNA encoding the reporters was spotted on LabTek chambered coverglass enabling reverse transfection of cells (Figure 1b). Images of expressing cells were acquired by semiautomated microscopy and analyzed to identify the sensor with the largest dynamic range (Figure 1c, d).

Several versatile cloning strategies for the generation of FRET reporters have been introduced recently.^{4,8} We were aiming for an even more flexible approach permitting unrestricted exchange of all construct components. First, we designed basic FRET backbone plasmids containing different donor–acceptor combinations. mECFP, the recently developed mTurquoise,⁹ and mTurquoiseDEL, lacking the C-terminal 11 amino acids, were used as donors. The yellow fluorescent protein Venus and its circularly permuted variants cp49Venus, cp157Venus, cp173Venus, and cp229Venus³ were used as acceptors. The linker sequence between fluorescent proteins and the protein of interest may determine FRET performance. Longer linkers will likely increase the structural flexibility of the sensor and may ensure sufficient orientations in which FRET is permitted. Shorter linkers sometimes fix a favorable (or unfavorable) FRET orientation and may produce particularly good or bad FRET. Therefore, donors and acceptors were separated from the insert by two, four, or eight amino acids. This resulted in a FRET backbone library that, while being small

Received: December 8, 2010

Accepted: April 20, 2011

Published: April 20, 2011

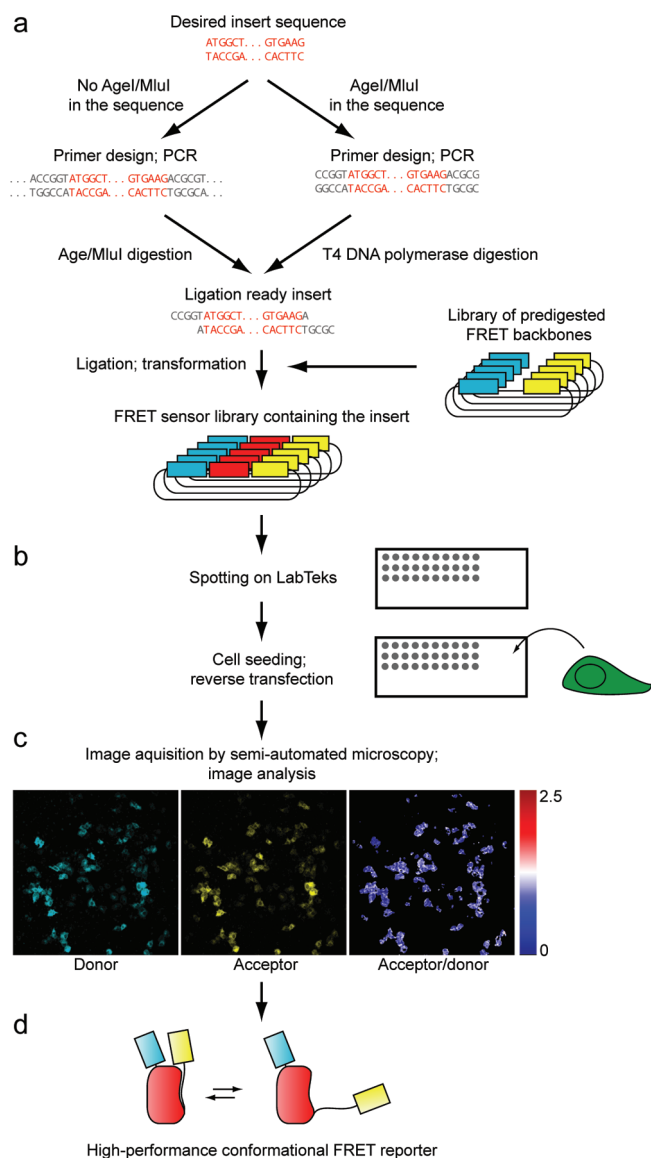


Figure 1. Workflow for the development of genetically encoded FRET reporters. (a) A library of constructs was cloned consisting of different FRET donor/acceptor pairs connected to the desired insert by variable linkers. (b) Plasmid DNA was spotted on LabTek coverglass to enable reverse transfection of cells. (c) Images were acquired by semiautomated microscopy and analyzed. (d) Single best performing conformational FRET reporter was selected for follow-up studies.

enough to be easily handled (36 plasmids), still contains variability in all factors critical for FRET. Unique restriction sites were used to build the plasmids, allowing for easy exchange of donor, acceptor, and linker sequences. For inserting any desirable sequence into the backbones, we chose AgeI and MluI, which enable restriction enzyme cloning, provided that the restriction enzyme recognition sites are not present in the desired sequence. In case restriction enzyme cloning cannot be used due to the presence of AgeI or MluI recognition sites, sticky ends may be generated by 3'→5' exonuclease activity of T4 DNA polymerase, similar to ligation independent cloning. However, the inserts are still ligated into the backbones by use of the T4 DNA ligase (Figure 1a). A detailed depiction of the FRET construct organization can be found in Supplementary Figure 1.

To validate the approach, we decided to generate sensors for two calmodulin-binding proteins, Camk2a and DAPK1, a Ser/Thr kinase implicated in cancer.¹⁰ Recently, the crystal structure of the DAPK1–calmodulin complex was solved and suggested a large conformational shift of the kinase upon calmodulin binding.⁷ The fragment consisting of amino acids 1–334 used to determine the structure was chosen as a starting point for the design of FRET reporters. We prepared 36 DAPK1 1–334 constructs using the FRET backbone plasmids listed in Figure 2a. The complete list of available FRET constructs, including some not used in this study, can be found in Supplementary Table 1. The 36 DAPK1 constructs were then printed on LabTek chambered coverglass. The advantage of this approach is that the arrays can be stored for many months and that all cells will receive the same treatment under identical conditions.^{11,12}

HeLa cells were seeded in prepared LabTek chambers and reversely transfected within 20–24 h. Transfection efficiency ranged from 5% to 40% in most spots. The transfected spots were imaged by semiautomated microscopy. Cells were monitored before and after addition of the calcium ionophore ionomycin, and the acceptor/donor ratios were calculated. The ratio change for each sensor is shown in Figure 2b. The best performing reporter, DAPK1(334)-F40, consisting of mTurquoise and cp173Venus with two amino acids between the fluorescent proteins and the DAPK1 fragment, showed a 55% decrease in FRET. Comparison of all sensor candidates indicated that mTurquoise was a significantly better FRET donor than ECFP as was previously demonstrated by FLIM/FRET analysis.⁹ Diverse permutations of the acceptor performed differently, with cp173 being the best in this example. The shortest linker was best in most cases, most likely because it shortened the fluorescent protein distance, reduced their tumbling freedom and allowed for fluorescent protein orientation effects to become more pronounced. The use of dimerizing varieties of the fluorescent proteins did not improve sensor performance as was described for other FRET sensors,¹³ probably due to too large distances between the β -barrels (Supplementary Figure 2a, b). Additional circular permutations of Venus, such as cp145Venus and cp195Venus, also failed to increase the dynamic range of the sensor (Supplementary Figure 2a, b).

Next, 30 sensors containing full-length (1–478) rat Camk2a (excluding constructs with mECFP as donor) were prepared, printed, and analyzed as described above. In addition, 10 sensors comprising the 1–328 fragment of Camk2a were produced. This fragment, containing the catalytic and autoregulatory/calmodulin binding domain, was equivalent to the 1–334 fragment of the DAPK1, as predicted by using structurally assisted sequence alignment (Supplementary Figure 3). Due to high structural similarity between the two kinase fragments, only the 10 FRET backbones with 2 amino acids linkers were chosen as they performed best for DAPK1. HEK-293 cells were used due to poor transfection efficiency of HeLa cells in these two batches of spotted LabTek dishes. In contrast, transfection efficiency of HEK-293 cells mostly ranged between 20% and 80%. When used in liquid transfection experiments, the same plasmid DNA samples worked equally well with both cell types. We conclude that although the method may be fairly robust, certain variability can be expected between spotting batches and also between samples of a single batch if they are manually prepared. The semiautomated scanning of LabTek dishes printed with full length Camk2a sensors revealed Camk2a-F63 as the sensor exhibiting the largest FRET ratio change (Figure 2b). However,

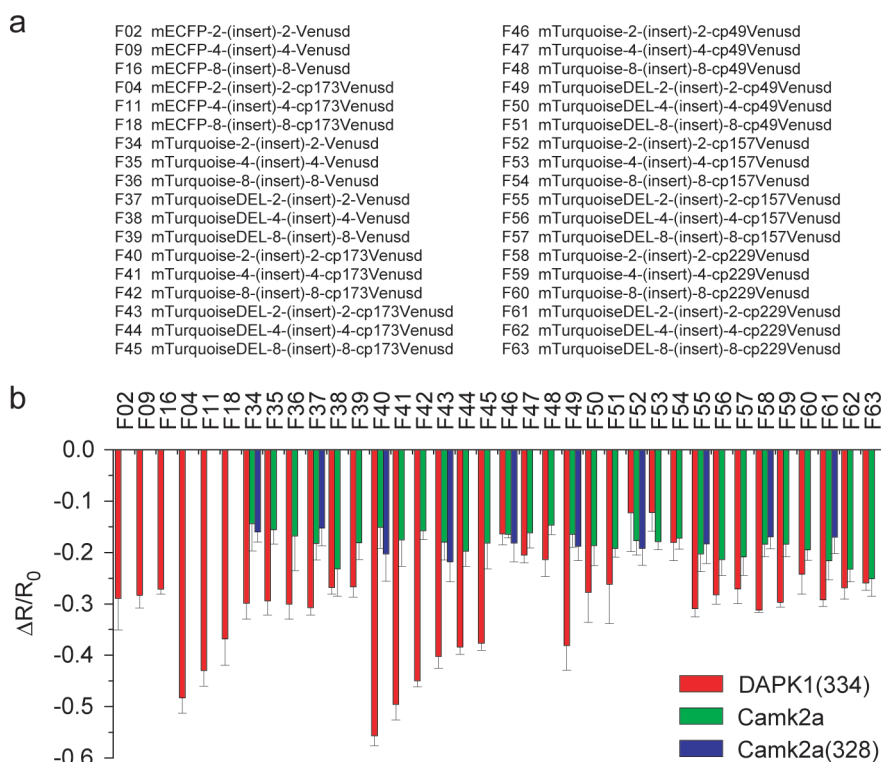


Figure 2. Overview of the FRET construct library and performance of DAPK1 and Camk2a sensors. (a) List of 36 FRET vectors used in this study. *d* = dimerizing, A206; *m* = monomeric, A206K. (b) Change of acceptor/donor emission ratio: 36 sensors containing the 1–334 fragment of DAPK1 expressed in HeLa cells (shown is the mean and SD of 3 scanned dishes); 30 sensors containing full length Camk2a expressed in HEK-293 cells (5 scanned dishes); 10 sensors containing 1–328 fragment of Camk2a expressed in HEK-293 cells (5 scanned dishes).

the dynamic range of this sensor was much smaller than that of the best DAPK1 reporter and the differences between all sensors were less pronounced, with performance ranging between 15% and 25% decrease in acceptor/donor ratio. Similar results were achieved with Camk2a 1–328 sensors (Figure 2b). Given the predicted structural similarity between the 1–334 fragment of the DAPK1 and 1–328 fragment of the Camk2a, this difference in sensor performance was unexpected. One possible explanation is that conformation and position of the short and terminal unstructured regions may be different in both kinases, resulting in higher flexibility in the case of Camk2a and neutralization of the influence different fluorescent protein geometries may have on FRET.

With the goal to further increase the dynamic range of the sensors, we truncated the C terminus of DAPK1(334)-F40 and Camk2a(328)-F40 inserts, as the initial sequences contained 14 amino acids not required for calmodulin binding and not observed in the crystal structure (PDB ID 2X0G). For the DAPK1 sensor, progressive removal of the C-terminal amino acids did not result in a significant performance improvement (Supplementary Figures 4a and 4b). However, the Camk2a truncation led to an increase in FRET change. In low-throughput experiments in HeLa cells, Camk2a(314)-F40 showed an ~5% larger drop in total acceptor/donor ratio than the original Camk2a(328)-F40 sensor. Camk2a(314)-F40 was therefore chosen for further analysis. The results are shown in Supplementary Figure 4c, d. Supplementary Figures 4e, f also contain a comparison of the best full-length Camk2a-F63 sensor identified using the library approach to the previously used, randomly designed Camk2a sensor CYCaMIII α .¹⁴

We next used the three best sensors, DAPK1(334)-F40, Camk2a(314)-F40, and Camk2a-F63, and monitored their activation in low-throughput time lapse microscopy experiments. HeLa cells expressing DAPK1(334)-F40 and the corresponding acceptor/donor ratio images from such experiments are shown in Figure 3a. The localization of DAPK1(334)-F40 and Camk2a-F63 was cytoplasmic, whereas Camk2a(314)-F40 was also present in the nucleus (data not shown). Sensor performance was similar to that seen in the semiautomated microscopy approach, with DAPK1-F40 showing around 60% decrease in acceptor/donor ratio, while the two Camk2a reporters showed a decrease of about 30% (Figure 3b). Apart from the onset of activation, which may vary due to inconsistencies in the manual addition of the ionophore, the three sensors appeared to have very similar and rapid activation kinetics. Moreover, since all low-throughput microscopy experiments were performed in HeLa cells, we confirmed that the differences in performance of the DAPK1 and Camk2a sensors observed in semiautomated scanning experiments in HeLa and HEK-293 cells were not due to the use of different cell types. In fact, the experiments shown in Figure 3a suggest that the difference originates from the higher starting FRET values of the DAPK1 sensor, while the final FRET values appear to be very similar.

We therefore performed acceptor bleaching analysis of the three sensors and determined FRET efficiencies before and after ionomycin stimulation of sensor expressing cells. An example of HeLa cells expressing DAPK1(334)-F40 and a FRET efficiency image from an acceptor bleaching experiment is shown in Figure 4a. The experiments confirmed the difference in performance between

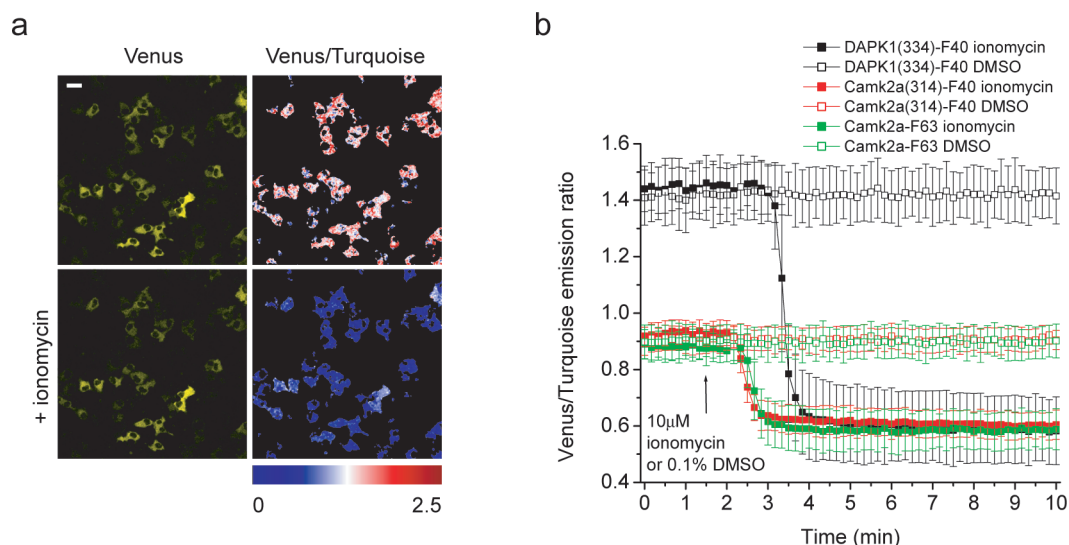


Figure 3. Low-throughput ratiometric analysis of the best performing DAPK1 and Camk2a sensors identified by LabTek scanning. (a) Images of HeLa cells expressing DAPK1(334)-F40 and calculated acceptor/donor ratio images with the corresponding LUT before and after addition of ionomycin. Scale bar, 30 μm. (b) Acceptor/donor ratio changes over time are shown for the three sensors expressed in HeLa cells and treated with ionomycin or DMSO (mean ± SD, $n = 27–57$ cells).

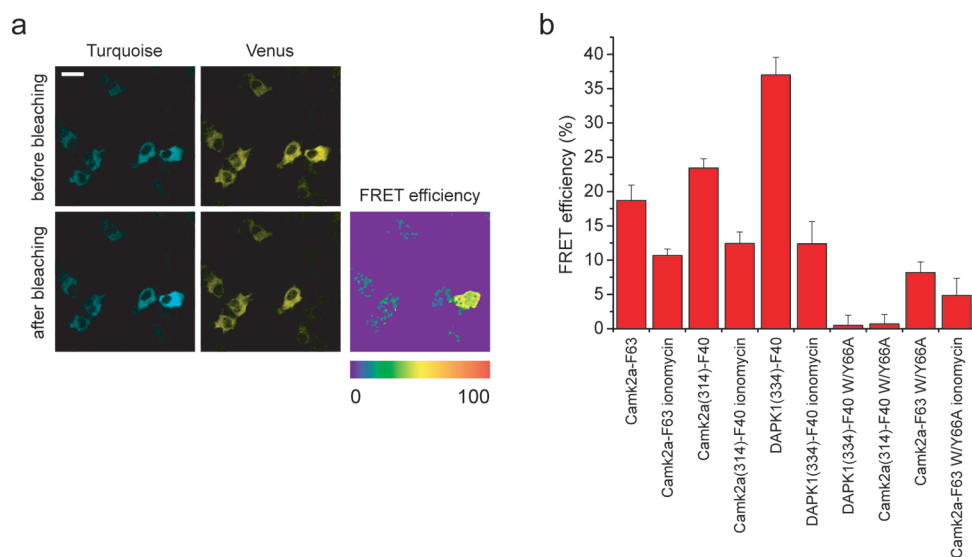


Figure 4. Acceptor bleaching FRET analysis of the best performing DAPK1 and Camk2a sensors. (a) Images showing HeLa cells expressing DAPK1-F40 before and after acceptor bleaching and calculated FRET efficiency image with the corresponding LUT. Scale bar, 30 μm. (b) FRET efficiency values of the three sensors before and after ionomycin stimulation. Additionally, FRET is shown in cells co-expressing non-fluorescent mTurquoise and Venus variants of the same sensors to reveal the intermolecular contribution to FRET (shown is mean ± SD, $n = 8–11$ measurements).

the DAPK1 and the two Camk2a sensors (Figure 4b). They also showed that after full stimulation the sensors still exhibited more than 10% FRET efficiency. Using the acceptor bleaching technique, we also tested for the intermolecular contribution to the FRET signal. For that purpose, we created non-fluorescent donor and acceptor point mutants for each of the reporters. In HeLa cells co-expressing a non-fluorescent donor variant of a sensor together with a non-fluorescent acceptor variant of the same sensor, intermolecular FRET was measured. We found no significant intermolecular FRET in the case of DAPK1(334)-F40 or Camk2(314)-F40, confirming that the two sensors were acting truly intramolecularly. As expected, full length Camk2a-F63 with

its association domain and ability to oligomerize in HeLa cells¹⁵ exhibited significant intermolecular FRET (Figure 4b). Moreover, the use of non-fluorescent proteins in this experiment reduced the theoretically maximal FRET efficiency to 50% of the original sensor. Therefore, it appears that FRET in Camk2a-F63 is largely intermolecular and that the observed changes are most likely caused by conformational changes of the oligomeric Camk2a structure.⁶

As mentioned above and shown in Figure 3b, the timing of activation between the three sensors appeared to be similar. We therefore performed intracellular calcium measurements with the calcium indicator Fura red in parallel to ratiometric FRET

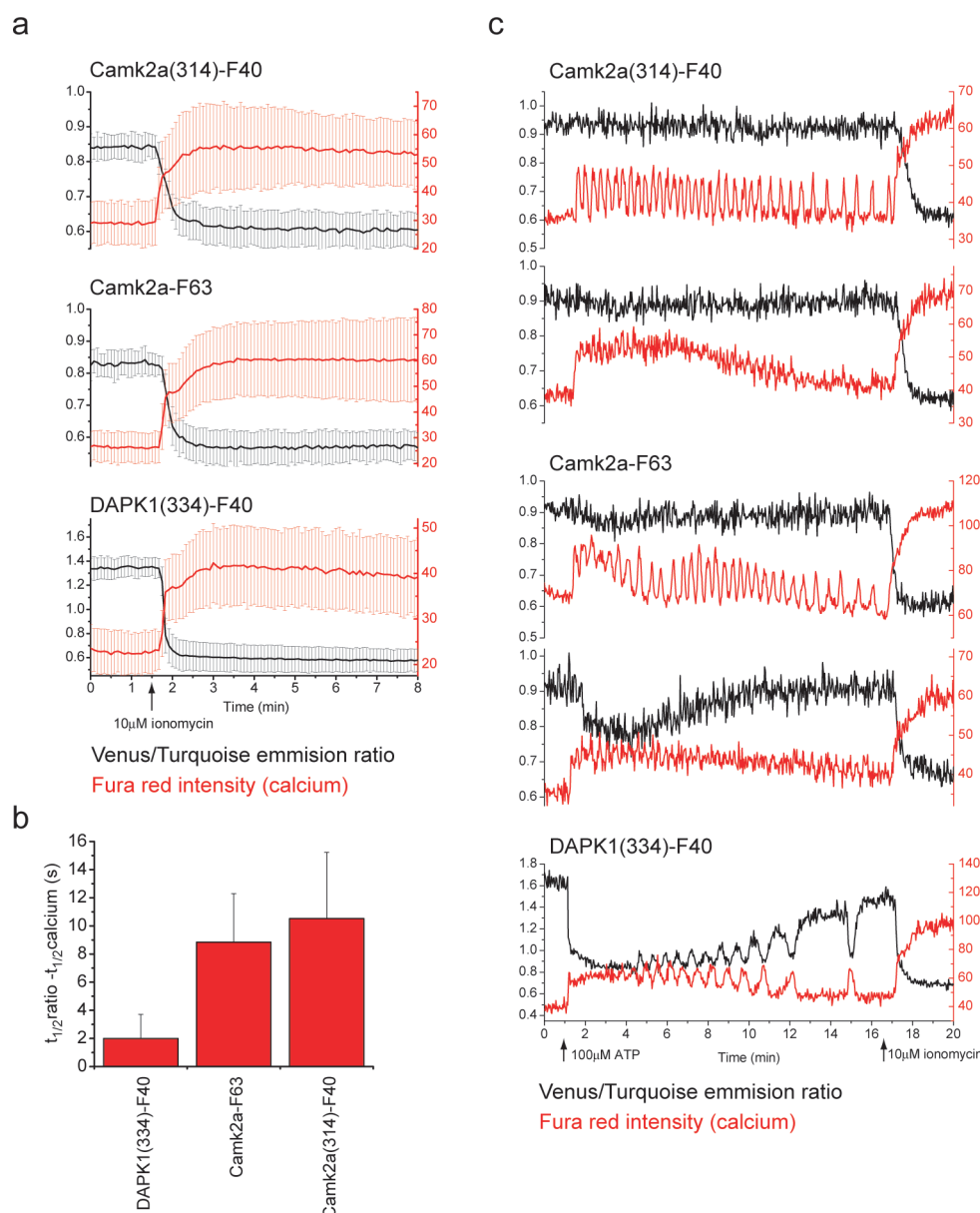


Figure 5. Simultaneous ratiometric FRET and calcium measurements. (a) DAPK1 and Camk2a sensors measured in parallel with the calcium indicator Fura red in HeLa cells stimulated with ionomycin (mean \pm SD, $n = 29-43$ cells). (b) Time differences in the half-times of enzyme activation and calcium responses derived from individual cells traces of experiments shown in a (mean \pm SD). (c) Representative single cell traces of the FRET sensors measured in parallel to calcium in HeLa cells stimulated with ATP followed by ionomycin. At least 25 cells were measured in each experiment. DAPK1 oscillations were observed in all cells that exhibited calcium spiking.

measurements. The dynamics of the calcium signal was used as a reference to determine how fast the conformational changes in the three reporters were occurring in response to elevated calcium levels (Figure 5a). We determined that the conformational change of DAPK1(334)-F40 occurred with a mere 2.0 ± 1.7 s ($n = 34$) delay after the ionomycin-induced calcium increase. In contrast, Camk2a-F63 and Camk2a(314)-F40 were delayed by 8.8 ± 3.4 s ($n = 43$) and 10.5 ± 4.7 s ($n = 29$), respectively (Figure 5b).

We finally tested all three reporters in parallel to calcium measurements in HeLa cells stimulated with $100 \mu\text{M}$ ATP (Figure 5c). ATP induced either repetitive calcium spiking or single calcium transients in all experiments as demonstrated by Fura red intensity traces. While Camk2a(314)-F40 did not

respond to ATP stimulation, Camk2a-F63 showed a transient conformational change after calcium transients, but lacked the response to oscillatory calcium spiking. In contrast, DAPK1-F40 reacted to calcium spiking demonstrating its capacity to detect even fairly small and short-lived changes in calcium levels and to translate them into oscillatory kinase behavior. These differences between DAPK-1 and Camk2a may depend on a variety of factors, including differences in calcium/calmodulin binding and additional post-translational modifications. Further investigations are necessary to determine the regulation of the various kinase response patterns.

In conclusion, we developed a highly flexible method for efficient production of genetically encoded FRET sensors. Once the basic set of 36 constructs was prepared, preparation of new

constructs was fast (about two weeks) and the following two steps of DNA spotting and subsequent microscopy were performed within a few hours each. We used the approach to create DAPK1 and Camk2a reporters useful to study signal transduction events controlled by calcium/calmodulin and the associated regulatory mechanisms. For future cell biology applications, it will now be possible to study the translation of lasting, transient, and oscillatory calcium signaling into the downstream responses at the protein level. Additionally, the DAPK1 reporter is one of the few genetically encoded FRET sensors that exhibits a sufficiently large FRET change for successful screening of small compound libraries in living cells. From the technical side, we obtained insights into FRET sensor design rules. In particular, we conclude that the choice of different circularly permuted fluorescent proteins may have a greater impact on sensor performance than small differences in fluorophore-insert linker lengths. In the future, the current library could be further expanded to include additional geometries between the fluorescent proteins and the insert of choice. For instance, the use of circularly permuted fluorescent FRET donor proteins could be added to the library. Independent of library size, we believe the method described here provides a fast and general way to optimize FRET sensors with a modest effort but a high rate of success especially for the many calmodulin-binding proteins. In addition, the transfection and imaging approach will be essential for the future development of larger FRET sensor collections. The latter will be a crucial contribution to efforts in systems biology that are in great need of validating cell models by live cell experiments on a much broader level than currently possible.

METHODS

Cloning. FRET construct backbones were prepared by amplification of individual components and their assembly into the pECFP-C1 (Clontech) vector. Constructs with 2 amino acid linkers between the insert and the donor/acceptor were prepared by PCR amplifying the donor and inserting it into the pECFP-C1 using NheI and BglII. At the same time, the AgeI site in the plasmid sequence was removed and inserted in front of BglII. The acceptor was inserted using KpnI and BamHI with the MluI site introduced by PCR just after KpnI. Constructs with 4 or 8 amino acids linkers between the insert and the donor/acceptor were prepared by first inserting the donor using NheI and BglII (AgeI site in pECFP-C1 removed), followed by insertion of the acceptor using KpnI and BamHI site. Four or 8 amino acids linkers were introduced by oligonucleotides designed to contain AgeI and MluI sites, flanked directly with BglII and KpnI sites in case of 4 amino acid linker constructs or with BglII and KpnI and 12 more nucleotides in case of 8 amino acids linker constructs. The oligonucleotides were phosphorylated, annealed, and ligated into the donor- and acceptor-containing vectors described above. The schematic view of the composition of the resulting constructs is shown in Supplementary Figure 1. Libraries of FRET constructs containing human DAPK1 (NM_004938) or rat Camk2a (NM_012920) were generated by PCR amplifying the desired sequences and subsequent digestion of inserts, as well as destination FRET backbones with AgeI and MluI, and their subsequent ligation. Only restriction enzyme treated inserts were used, as in initial experiments this strategy yielded a higher number of transformed bacterial colonies than the T4 DNA polymerase strategy. It should be noted that in unpublished work we also used T4 DNA polymerase treated inserts to successfully prepare FRET constructs. Fluorescence inactivating mutations (W66A for mTurquoise and Y66A for Venus) were introduced using the Stratagene QuikChange site directed mutagenesis kit according to the manufacturer's instructions.

Plasmid DNA Spotting. Plasmid DNA spotting solution was prepared manually similarly to a previously reported method.¹¹ Three microliters of 0.4 M sucrose (USB) in OptiMEM (Gibco) was mixed with 3.5 μ L of Lipofectamine 2000 (Invitrogen) and 2 μ g of plasmid DNA in a 384-low volume well plate (Nunc). The solution was incubated for 20 min at RT. Then, 7.25 μ L of a 0.2% (w/v) gelatin (Sigma-Aldrich) solution containing 1 \times 10⁻³ % (w/v) fibronectin (Sigma-Aldrich) was added to each well. The transfection solution was printed on LabTek chambered coverglass (Nunc) using the contact printer ChipWriter Pro (Bio-Rad) with solid pins PTS 600 (Point Technologies). Spots were 400 μ m in diameter and 1500 μ m apart. Each FRET construct was printed in triplicate per LabTek coverglass. Sixteen LabTek replicates were printed for each set of FRET constructs (36 DAPK1(334) reporters, 30 Camk2a and 10 Camk2a(328) reporters were spotted on a separate batch of LabTek dishes, respectively). After spotting, LabTek dishes were placed in a box containing drying pearls (Fluka) and stored at RT for at least 24 h before cell seeding.

Cell Culture and Transfection. All cell experiments were performed with HeLa Kyoto or HEK-293 cells. HeLa cells were passaged and maintained in DMEM (Gibco) supplemented with 10% FBS (Gibco) and 0.1 mg mL⁻¹ primocin (Invivogen). HEK-293 were grown in DMEM with 4.5 g L⁻¹ glucose (Gibco), 10% FBS, 1 mM sodium pyruvate (Gibco) and 0.1 mg mL⁻¹ primocin. For LabTek scanning, 4–5 \times 10⁵ cells were seeded in each dish 20–24 h before imaging. For low throughput imaging experiments, cells were plated in 35 mm MatTek chambers (MatTek Corporation) and transfected at around 50% confluency with FuGENE 6 reagent (Roche). Transfections were performed in Opti-MEM (Gibco) according to the manufacturer's instructions. Cells were gently washed 20–24 h after transfection and incubated in imaging medium (20 mM Hepes, pH 7.4, 115 mM NaCl, 1.2 mM CaCl₂, 1.2 mM MgCl₂, 1.2 mM K₂HPO₄, 2 g L⁻¹ D-glucose) at 37 °C with 5% CO₂ for at least 15 min before imaging (1 h in case of LabTek dishes). A DMSO stock of ionomycin (Calbiochem) was prepared, and ionomycin was diluted in imaging medium before it was carefully added to the dish to give a final concentration of 10 μ M. ATP (Sigma-Aldrich) was dissolved in water and added at a final concentration of 100 μ M.

Microscopy. All experiments were performed on a Leica TCS SP2 AOBs microscope (Leica Microsystems) at RT. Excitation and emission settings were kept constant for ratiometric FRET analysis in order to image cells expressing similar amounts of the sensors and avoid expression related variability. Taking into account that intracellular sensor concentration should not exceed that of endogenous calmodulin, only medium expressing cells were measured. The 405 nm laser was used for excitation. Donor emission was sampled between 470 and 510 nm, acceptor emission between 520 and 540 nm. For LabTek scanning, we used an HC PL APO 20x/0.7 air objective. The pinhole was fully opened, images recorded in 8 bit mode with 2 lines averaging. Position and focus of one of three spots printed for each FRET construct, the one with the highest transfection efficiency, was manually marked. LabTek dishes were then automatically scanned before and 5, 10, and 15 min after addition of ionomycin. The first and last scans were used to calculate the sensor performance (see below). For low throughput microscopy, we used an HCX PL APO lbd.BL 40.0x/1.40 oil objective. The pinhole was half-opened (2.62 airy). Images were taken in 8 bit mode, with 1–2 line averaging and 2–10 s between frames. In acceptor bleaching FRET experiments, excitation and emission settings were donor exc 458 nm, em 470–500 nm; acceptor exc 515 nm, em 530–600 nm. The pinhole was fully opened. The acceptor was bleached with the 515 nm laser line in 2–3 iterations. Donor emission was measured before and after bleaching of the acceptor. FRET efficiency was calculated as described before.¹⁶ For calcium imaging experiments, 2 μ M Fura red/AM from Molecular Sensors (Invitrogen) was loaded into cells for 5 min. Cells were then gently washed and incubated in fresh

imaging medium for at least 15 min before image acquisition. Fura red was also excited with the 405 nm laser line and emission was sampled from 625 to 725 nm. Both donor and acceptor images were corrected for the Fura red bleed through before ratio calculation.

Image Processing and Analysis. All image processing and calculations were performed using ImageJ (<http://rsb.info.nih.gov/ij/>). Background levels were measured outside cells and subtracted globally. The median filter (1–2 pixel) was used for image smoothening. A threshold was applied before calculation of acceptor/donor ratio or FRET efficiency. Finally, LUT was applied to acceptor/donor ratio and FRET efficiency images. In the case of LabTek scanning, the mean ratio value of the entire field of cells before and after treatment was measured (one measurement per spot) and used to calculate the change of acceptor/donor ratio. In low-throughput time-lapse microscopy analysis individual cell traces were obtained. In multiparameter experiments, sigmoidal fits were used to obtain half-times of activation of individual reporters. Those values were used to calculate the difference in timing of sensor activation.

■ ASSOCIATED CONTENT

S Supporting Information. This material is available free of charge *via* the Internet at <http://pubs.acs.org>.

■ AUTHOR INFORMATION

Corresponding Author

*E-mail: schultz@embl.de.

■ ACKNOWLEDGMENT

We thank EMBL's Advanced Light Microscopy Facility for support, B. Neumann and J. Bulkescher for technical advice and assistance with plasmid DNA spotting, H. Stichnoth for cultured cells, D. Gadella for mTurquoise, and A. Miyawaki for Venus and circularly permuted Venus fluorescent proteins. Part of this work was supported by the Helmholtz Association (SBCancer).

■ REFERENCES

- (1) Chalfie, M., Tu, Y., Euskirchen, G., Ward, W. W., and Prasher, D. C. (1994) Green fluorescent protein as a marker for gene-expression. *Science* 263, 802–805.
- (2) Miyawaki, A. (2003) Visualization of the spatial and temporal dynamics of intracellular signaling. *Dev. Cell* 4, 295–305.
- (3) Nagai, T., Yamada, S., Tominaga, T., Ichikawa, M., and Miyawaki, A. (2004) Expanded dynamic range of fluorescent indicators for Ca²⁺ by circularly permuted yellow fluorescent proteins. *Proc. Natl. Acad. Sci. U.S.A.* 101, 10554–10559.
- (4) van der Krogt, G. N. M., Ogink, J., Ponsioen, B., and Jalink, K. (2008) A comparison of donor-acceptor pairs for genetically encoded FRET sensors: Application to the Epac cAMP sensor as an example. *PLoS One* 3, e1916.
- (5) Rellos, P., Pike, A. C. W., Niesen, F. H., Salah, E., Lee, W. H., Von Delft, F., and Knapp, S. (2010) Structure of the CaMKII delta/calmodulin complex reveals the molecular mechanism of CaMKII kinase activation. *PLoS Biol.* 8, e1000426.
- (6) Rosenberg, O. S., Deindl, S., Sung, R. J., Nairn, A. C., and Kuriyan, J. (2005) Structure of the autoinhibited kinase domain of CaMKII and SAXS analysis of the holoenzyme. *Cell* 123, 849–860.
- (7) de Diego, I., Kuper, J., Bakalova, N., Kursula, P., and Wilmanns, M. (2010) Molecular basis of the death-associated protein kinase-calcium/calmodulin regulator complex. *Sci. Signaling* 3, ra6.
- (8) Kotera, I., and Nagai, T. (2008) A high-throughput and single-tube recombination of crude PCR products using a DNA polymerase inhibitor and type IIS restriction enzyme. *J. Biotechnol.* 137, 1–7.
- (9) Goedhart, J., van Weeren, L., Hink, M. A., Vischer, N. O. E., Jalink, K., and Gadella, T. W. J. (2010) Bright cyan fluorescent protein variants identified by fluorescence lifetime screening. *Nat. Methods* 7, 137–139.
- (10) Gozuacik, D., and Kimchi, A. (2006) DAPk protein family and cancer. *Autophagy* 2, 74–79.
- (11) Erfle, H., Neumann, B., Liebel, U., Rogers, P., Held, M., Walter, T., Ellenberg, J., and Pepperkok, R. (2007) Reverse transfection on cell arrays for high content screening microscopy. *Nat. Protoc.* 2, 392–399.
- (12) Conrad, C., Erfle, H., Warnat, P., Daigle, N., Lorch, T., Ellenberg, J., Pepperkok, R., and Eils, R. (2004) Automatic identification of subcellular phenotypes on human cell arrays. *Genome Res.* 14, 1130–1136.
- (13) Kotera, I., Iwasaki, T., Imamura, H., Noji, H., and Nagai, T. (2010) Reversible dimerization of *Aequorea victoria* fluorescent proteins increases the dynamic range of FRET-based indicators. *ACS Chem. Biol.* 5, 215–222.
- (14) Piljic, A., and Schultz, C. (2008) Simultaneous recording of multiple cellular events by FRET. *ACS Chem. Biol.* 3, 156–60.
- (15) Piljic, A., and Schultz, C. (2008) Analysis of protein complex hierarchy in living cells. *ACS Chem. Biol.* 3, 749–755.
- (16) Wouters, F. S., Verveer, P. J., and Bastiaens, P. I. (2001) Imaging biochemistry inside cells. *Trends Cell Biol.* 11, 203–11.